Spray-coating deposition techniques for polymeric semiconductor blends

Bernardin, Gavin; Davies, Nathan; Finlayson, Christopher

Published in:
Materials Science in Semiconductor Processing

DOI:
10.1016/j.mssp.2017.07.026

Publication date:
2017

Citation for published version (APA):
Bernardin, G., Davies, N., & Finlayson, C. (2017). Spray-coating deposition techniques for polymeric semiconductor blends. *Materials Science in Semiconductor Processing*, *71*, 174-180. https://doi.org/10.1016/j.mssp.2017.07.026

Spray-coating Deposition Techniques for Polymeric Semiconductor Blends

Gavin A. Bernardin, Nathan Davies and Chris E. Finlayson*

Department of Physics, Prifysgol Aberystwyth University, Aberystwyth SY23 3BZ, Wales, UK.

*E-mail; cef2@aber.ac.uk

Abstract

We develop a universal method for spray-deposition of polymeric semiconductor blends, based on blends of polyfluorenes (F8TBT), polythiophenes (P3HT) and fullerenes (PCBM), as suitable for large areas. A multi-faceted characterisation approach, studying photoluminescence quenching, together with atomic force and optical microscopy, illustrates favourable results in terms of layer thickness, uniformity, and mesoscale morphology. With key engineering tolerances in mind, thermal (melt) and solvent-vapour annealing are investigated as post-processing methods, for improving the planarity of craterform layers and blend photophysical characteristics.

Keywords

Spray-coating, polymer blends, annealing methods, thin-films, conjugated polymers

1. Introduction

Organic/polymeric solar cells offer a promising route towards low-cost renewable energy production [1-3]; however, large-area mass production techniques still represent a significant scientific and engineering challenge. For many years, spin-coating has been the benchmark technique by which the composite thin-laminar layers of optoelectronic devices have been deposited over length scales of up to 10s of cms [4-6]. In addition to the limitations of workable deposition area, a large fraction of the active materials are unavoidable wasted during the process. Because of the different associated challenges with, for example, building-integrated photovoltaics (BIPVs), new manufacturing processes have to be developed, including techniques originally invented for printing or painting of large areas and diverse shapes.

A pneumatically driven ejection mechanism ("spray gun"), is a ubiquitous tool familiar from everyday life, spray-painting being one particular example. The solubility of polymeric semiconductors in a range of solvents, and the resultant solution-processability, make them highly compatible with such a method. The processing is easily scalable, and uses materials far more cost-efficiently than spin coating. This method also does not depend on the surface of the substrate being planar, nor smooth at macroscopic levels. Commercially available kits, with considerable levels of control and variability, may thus be used for the deposition of thin-films and blend heterojunctions for potential device applications. Indeed, preliminary reports into the feasibility of spray-coated solar cells have yielded some promising results regarding device performance and stability [7-11]. Some attempts at using spray-coated active layers in polymeric transistors and field-effect transistors are also reported [12]. However, the main apparent drawback of this method is the roughness of the surface after coating, as illustrated by our earlier studies of polyfluorene photovoltaic blends [13]; the droplets formed in spray atomization translate into crater-like (or "craterform") structures in films on substrates, with relatively flat central areas and markedly raised edges or "walls". Of a particular prescience, the engineering tolerance of active layer thicknesses in organic optoelectronics range from a maximum of 1 micron for LEDs [14] down to sub-100nm in virtually all feasible solar cell designs. The relative lack of qualitative reports and quantitative analyses of these sprayed-film structures forms the basis for this additional research into generalised methods using a more complete range of solution-processable semiconductors, and into the effects of post-process annealing methods on the key characteristics of film roughness and photophysics.

In this paper, we thus examine the morphological characteristics and photophysical functionality of semiconductor thin-films, based on blends of key target materials, polyfluorenes (F8TBT), polythiophenes (P3HT) and fullerenes (PCBM), using a universal spray-coating deposition technique suitable for large areas. We further report a multi-faceted characterisation approach, studying blend photoluminescence (PL) quenching, optical microscopy, and thermal (melt) and solvent-vapour (SVA) post-annealing of films. Continuous macroscopically uniform thin-films, with highly distinctive mesoscale craterform structures, are demonstrated using these methods across all the blend systems studied. As a measure of the efficacy of charge separation at heterojunction interfaces, PL quenching efficiency of the as-deposited blends is studied before and after the application of post-process annealing. Finally, the planarity of blend films at the ~100nm height scales as inferred from microscope images and AFM data, is studied under the action of melt treatment.

2. Methods

The key interfacial energetics (see Figure 1b) illustrates the generic donor-acceptor nature of photovoltaic blends of P3HT, F8TBT, and PCBM [15]. This study explore the structures and photophysical properties characteristic of spray-coated films of the three blend permutations; namely P3HT/F8TBT, F8TBT/PCBM and P3HT/PCBM.

As illustrated in Figure 1, a double-action, siphon-feed spray gun (Wiltec type 128) is used for sample preparation, with working compressed air pressure range 1.0 - 3.4 bar and nozzle diameter 0.35 mm. In siphon-feeding, the solution is drawn upward by the air pressure gradient from a cup underneath the gun. This commercial spray-gun apparatus is limited in operation, in that the nozzle diameter (and spray-cone profile) is fixed, although a limited amount of adjustment is possible with the flow rate and the compressed-gas supply pressure. Adjustable experimental parameters are flow rate, solvent (and hence viscosity), material concentration, nozzle-substrate distance (X), substrate temperature. In terms of the optimal solvent media parameters for deposition of these materials, we adopt the approach of Noebels *et al*.[13], using a solvent mixture of low viscosity chlorinated-aromatic solvents. We find that the optimal conditions of droplet size, solution transfer, substrate adhesion, and film formation can be obtained using a mixture of chlorobenzene(CB) and dichloro-benzene(DCB) in a 1:5 ratio (all solvents from Sigma-Aldrich); this solvent medium has a measured dynamic viscosity of 1.22 cP. According to specifications, all parts of the airbrush are known to be resistant

against these solvents. The materials used in the preparation of blend films, namely poly(3-hexylthiophene) (P3HT) and phenyl-C61-butyricacidmethylester (PCBM), were obtained from Sigma Aldrich. Poly[(9,9-dioctyluorene)-2,7-diyl-alt-(4,7-bis(3-hexylthien-5-yl)-2,1,3-benzothiadiazole)-2′,2″-diyl] (F8TBT) was obtained from the Melville Laboratory, Cambridge [16]. We find subsequently that the method can be universally used for blend combinations of F8TBT, P3HT and PCBM, as deposited onto cleaned quartz (spectrosil) substrates.

As will be discussed below, solution droplet sizes in the range of radius ~10-100 μm may be inferred, as is consistent with a so-called *fine atomization* regime of spray-coating [17, 18]. Our measurements indicate that at the relevant values of solvent viscosity, the controllable flow rates can be adjustably set to either 8, 21 or 59 microlitres/sec at 1.4 bar, corresponding to nozzle velocities of 26, 52 and 78 m/s respectively. The flow rate of 21 μl/sec is typically chosen, with X ~10-20 cm, and polymer concentration ~ 1 mg/ml, giving film deposition rates of order 200 nm/min. Pre-optimized substrate temperatures of $T \approx 80°C$ induce sufficiently rapid evaporation of the solvent, leaving permanently formed structures. This approach enables samples to be generated either from a single deposition step or from multiple deposition cycles. A further study may be justified to determine if this would enable, for example, multilayer bulk-heterojunction structures to be discretely deposited. Multiple samples were generated of each blend type within the present study, in ~1:1 weight component ratios, to allow evaluation of reproducibility and reliability of both the method and the characteristic properties of films. Whilst substrates of area ~1cm^2 are coated and studied here, the set-up will readily and uniformly coat an area of up to 15-20 cm in diameter, if required.

Subsequent characterisation of samples involved multiple methodologies. AFM measurements of film morphology and tomography were taken over (40 x 40 μm) areas, using specially designed low frequency tips for soft matter samples (ND-MDT, Scanwel Ltd). Optical micrographs were obtained using a calibrated Meiji MX9000 series instrument in transmission mode. Optical absorption spectra of thin-film samples were recorded using an Ocean Optics Red-Tide integrated spectrophotometer. Photoluminescence (PL) measurements were taken using a $\lambda = 473$nm diode-pumped solid state laser (power of ~2 mW) as excitation source, combined with an Ocean Optics USB2000 fibre-coupled CCD spectrometer, with additional quantitative PL-quenching measurement being taken using a self-consistent "integrating sphere" method [19].

3. Results and Discussion

As a preliminary comparison with the more widespread method of spin-coating, in Figure 2 some very significant morphological differences with spray-coated blend films are already noted. These differences are subjectively obvious even in an optical microscope at low magnification. Invariably, with spin-coating a rather more optically flat uniform coating is produced over the small area of the substrate. However, this particular choice of solvent medium and (low) weight-concentration for spin-coating is evidently sub-optimal for the P3HT/PCBM and F8TBT/PCBM films, which suffer from some aggregate formation and incomplete film formation (tearing) respectively.

Figure 3 shows how, in both optical microscopy and AFM characterisation, continuous films are produced for each of the blend systems studied; the resultant mesoscale film morphologies consistently all show patterns of circular or elliptical craterform structures; typically 10-50 microns wide. Assuming the optimal conditions of drop adhesion and solvent evaporation to give film formation, as described in *Methods* above, we may estimate the corresponding droplet sizes produced by the spray-gun atomization process. If representative estimates for dried droplet radius (R) and thickness (t) of 10 μm and 150 nm respectively are used, then the volume of material in each craterform is given by $\pi R^2 t = 4.7 \times 10^{-17} m^3$. Taking a rough value for density of 1.5 g/cm^3, which is characteristic of polymer materials, this gives the mass of solid material in each droplet as being 7×10^{-11}g. Since typical solution concentrations used in spray-deposition here are 1 mg/ml, this gives a spherical drop volume ($4\pi r^3/3$) of 7×10^{-8} ml, and a drop radius, r, of order 25 μm within the fine atomization regime. Whilst the above calculation allows an estimation of droplet size, it has limitations in that it does not allow an accurate value of the size distribution to be obtained. Methods such as phase-Doppler anemometry (PDA) are widely reported in the measurements of atomized sprays and aerosol droplet sizes [18], and would make for an insightful further study; however, we do not presently have access to these techniques. As described above, the compressed-gas supply pressure may also be varied from 1.0 - 3.4 bar. The nebulization of the solution into droplets occurs via collisions due to the gas flow turbulence; the surface energy of the solvent increases, producing small droplets. According to outline theory [20], where droplet size D goes as the gas pressure P, such that $D \sim P^{-0.3}$, we expect this to give mean particle radii ranging from approximately 19 up to 27 microns within the adjustable range. Hence, only a limited parametric study into droplet size is theoretically possible, and other optimization

considerations, where we must operate within a parametric range that gives tractable solvent transfer, film adhesion and formation ($P \approx 1.4$ bars) restrict this still further.

A more detailed analysis of the AFM images and data reveals crater-like ("craterform") structures with walls and more flat and uniform coating in the centers. Noting that wall heights of greater than ~100 nm may be problematic, given usual engineering tolerances in optoelectronic device processing, in Table 1 typical inferred high ranges and surface roughnesses are given for each of the blend systems studied. We find that all as-deposited films exhibit craterform wall heights in the range of ~ 90-110 nm, whilst the films containing F8TBT appear to show better "film-forming" behavior (i.e. lower roughness); a relatively high r.m.s. roughness of ~90nm is typically measured for P3HT/PCBM. At the available levels of resolution and scan areas, no clear evidence of phase separation of blend components is observed; as expected, any such separation apparently shows a much finer (sub-micron) morphology [21, 22]. We may now make some quantitative comparisons with other reports of spray-coating of polymer films from the literature. In Abdellah *et al*. [12], morphological characterisation of P3HT films as sprayed from toluene solution are likewise characterized as having r.m.s. roughnesses above 100 nm, as compared to below ~ 3 nm for optimally spin-coated films. In Hoth *et al*. [23], P3HT:fullerene blends are sprayed onto device substrates using various deposition strategies, with roughnesses of between 46 and 68 nm reported, in comparison to 3-4 nm for doctor-bladed thin-films. Without the same detailed attention paid to film morphology/roughness and post-processing as in the present study, these earlier reports nonetheless strongly corroborate both our qualitative (Figure 2) and quantitative (Table 1) findings.

The pristine F8TBT and P3HT films, as deposited by spray-coating show efficient photo-luminescence (PL) under blue/UV laser excitation; with values in the ranges of 10% and 4-5% respectively, in consistency with the literature [16, 24]. The as deposited 1:1 blends show a significantly reduced PL emission (Figure 4), as charge-separation at heterojunction interfaces now competes with radiative recombination (PL quenching); the degree of such quenching is also therefore an indicator of likely photovoltaic cell performance [22]. We may quantify the extent of PL quenching (η) by directly comparing the integrated emission intensity of blends with the that of the unblended pristine (reference) material; thus-

$$\eta = 1 - \frac{I_{blend}}{I_{ref}} \cdot \frac{A_{ref}}{A_{blend}}, \qquad \text{(eq.1)}$$

where I_{blend} and I_{ref} are the spectrally integrated luminescence intensities, and A_{ref} and A_{blend} are the measured film absorbances at the laser excitation wavelength. By this definition, complete quenching (where $I_{blend} = 0$) would correspond to $\eta = 1$, whereas a lack of any quenching (where $I_{blend} \approx I_{ref}$) would correspond to $\eta = 0$. As displayed in Table 2, PL quenching efficiencies ranging from 0.49 in P3HT/F8TBT to 0.96 in PCBM/F8TBT were typically measured for the as-deposited samples.

As a further study, thermal (melt) and solvent-vapour (SVA) annealing are used as post-processing methods of modifying and optimising the as-deposited films. These are methods which may be readily replicated and implemented in large-scale processing, giving extra control of the morphology and phase separation of blend components [25], and most critically in this context, the planarity of films on the substrate (see Figure 5 schematic). For thermal annealing, the samples were placed on a hot plate in air at 150°C for 20 minutes, and then allowed to cool for 40 minutes, cooling at a rate of 3.75°C per minute. These parameters were chosen to facilitate melt flow of the deposited film on the substrate, whilst avoiding any thermal decomposition or damage, as per earlier literature reports [26-28]. For SVA, we adopt well-established processing parameters used to alter or induce the desired phase separation in organic electronics, adopting chloroform as the common solvent for P3HT/PCBM/F8TBT co-blends [29]. The samples were kept in a chloroform rich (saturated vapour) environment for 30 minutes, within an enclosed chamber and chloroform reservoir gently heated to just above room temperature (≈ 30°C) to facilitate the solvent evaporation.

Table 2 illustrates how the PL quenching efficiency of blends improves more significantly with SVA, as compared to thermal annealing. Whilst η for the F8TBT/PCBM blend was already approaching complete quenching after deposition at 0.96, the increases with SVA in the other two systems were from $\eta = 0.49$ to 0.67 for P3HT/F8TBT and 0.77 to 0.88 for P3HT/PCBM. This is consistent with many previous reports of the effects of nanoscale morphology changes, leading to more effective exciton diffusion to domain interfaces (heterojunctions) [30-32]. Conversely, the observed planarity of blend films (Table 1) are significantly improved by thermal/melt treatment, but not by SVA. This may be inferred qualitatively from the optical microscope and AFM images in Figure 5; in particular, the walls associated with droplets appear more sunken and less raised from the substrate, corresponding to reductions in roughness of some 40-50%. Quantitatively analysis from the AFM data, shows reduced roughness in all cases, and a decrease of r.m.s. roughness of approaching 50% for

P3HT/F8TBT and P3HT/PCBM. In general, F8TBT/PCBM samples show little change from the as-deposited characteristics with either annealing treatment.

4. Conclusions

A universal method for pneumatic spray-deposition of polymeric semiconductor thin-films, based on blends of polyfluorenes (F8TBT), polythiophenes (P3HT) and fullerenes (PCBM), as suitable for large areas, has been developed. A multi-faceted characterisation approach, including detailed atomic force microscopy (AFM) studies, show that favourable results in terms of deposition layer thickness, uniformity, and mesoscale morphology can be achieved using mixtures of o-dichlorobenzene and chlorobenzene as the optimised solvent medium. Continuous thin-films of "craterform" 10-50 μm wide dried droplets are formed with notable wall structures and a more flat uniform coating in the centre. As a measure of the efficacy of charge separation at heterojunction interfaces, PL quenching efficiency of the as-deposited blends improves significantly with SVA, but not with thermal/melt annealing. Conversely, the planarity of P3HT/F8TBT and P3HT/PCBM films at the ~100nm height scales are significantly improved by melt treatment, but not by SVA, as inferred from microscope images and AFM data.

Thus, thermal (melt) annealing is shown as a tractable post-processing method for improving the planarity of craterform layers for potential optoelectronics applications. These are important findings in the context of key engineering tolerance parameters for planar device processing technologies. In terms of photophysical characteristics; high photoluminescence quenching efficiencies, indicative of effective charge separation at heterojunction interfaces, were typically measured for the as-deposited samples, with marked improvement upon the action of solvent-vapour annealing.

In addition to the ease of controllable large-area scalability, much improved cost-effectiveness of material use, and tractability of deposition on non-planar substrates, it should be possible to integrate the spray-coating and post-processing steps (heat/SVA) required into roll-to-roll style manufacturing arrays [33-35]. We anticipate that future development and engineering of such device manufacturing will also include studies into how non-chlorinated and less toxic solvents may be used, using the regimes of optimised viscosity and fine-atomization spray parameters developed here.

5. Acknowledgements

The authors acknowledge Sigma Aldrich and the Melville Laboratory, Cambridge [16] for the supply of materials used in this work, and Scanwel Ltd for technical support with AFM measurements. CEF thanks Mr Matthias Noebels for his preparatory work, forming the basis for this study. This research is supported by a *University Research Fund* (URF) award from Prifysgol Aberystwyth University.

References

[1] J. HALLS, C. WALSH, N. GREENHAM, E. MARSEGLIA, R. FRIEND, S. MORATTI, A. HOLMES, EFFICIENT PHOTODIODES FROM INTERPENETRATING POLYMER NETWORKS, Nature, 376 (1995) 498-500.
[2] J. Gao, G. Yu, A. Heeger, Polymer p-i-n junction photovoltaic cells, Advanced Materials, 10 (1998) 692-695.
[3] N. Sariciftci, Plastic photovoltaic devices, Materials Today, 7 (2004) 36-40.
[4] C. McNeill, N. Greenham, Conjugated-Polymer Blends for Optoelectronics, Advanced Materials, 21 (2009) 3840-3850.
[5] F. Krebs, Fabrication and processing of polymer solar cells: A review of printing and coating techniques, Solar Energy Materials and Solar Cells, 93 (2009) 394-412.
[6] S. Forrest, The path to ubiquitous and low-cost organic electronic appliances on plastic, Nature, 428 (2004) 911-918.
[7] G. Susanna, L. Salamandra, T. Brown, A. Di Carlo, F. Brunetti, A. Reale, Airbrush spray-coating of polymer bulk-heterojunction solar cells, Solar Energy Materials and Solar Cells, 95 (2011) 1775-1778.
[8] T. Wang, N. Scarratt, H. Yi, A. Dunbar, A. Pearson, D. Watters, T. Glen, A. Brook, J. Kingsley, A. Buckley, M. Skoda, A. Donald, R. Jones, A. Iraqi, D. Lidzey, Fabricating High Performance, DonorAcceptor Copolymer Solar Cells by Spray-Coating in Air, Advanced Energy Materials, 3 (2013) 505-512.
[9] R. Green, A. Morfa, A. Ferguson, N. Kopidakis, G. Rumbles, S. Shaheen, Performance of bulk heterojunction photovoltaic devices prepared by airbrush spray deposition, Applied Physics Letters, 92 (2008) 033301.
[10] D. Vak, S. Kim, J. Jo, S. Oh, S. Na, J. Kim, D. Kim, Fabrication of organic bulk heterojunction solar cells by a spray deposition method for low-cost power generation, Applied Physics Letters, 91 (2007).
[11] S. Tedde, J. Kern, T. Sterzl, J. Furst, P. Lugli, O. Hayden, Fully Spray Coated Organic Photodiodes, Nano Letters, 9 (2009) 980-983.
[12] A. Abdellah, D. Baierl, B. Fabel, P. Lugli, G. Scarpa, Exploring Spray Technology for the Fabrication of organic devices based on Poly(3-hexylthiophene), in: 9th IEEE Conference on Nanotechnology 2009, 2009, pp. 831-834.
[13] M. Noebels, R. Cross, D. Evans, C. Finlayson, Characterization of spray-coating methods for conjugated polymer blend thin films, Journal of Materials Science, 49 (2014) 4279-4287.
[14] L. Lu, C. Finlayson, R. Friend, Thick polymer light-emitting diodes with very high power efficiency using Ohmic charge-injection layers, Semiconductor Science and Technology, 29 (2014) 025005.
[15] C.R. McNeill, Polymers show versatility in organic solar cells, in, SPIE Newsroom, 2007.
[16] L. Lu, C. Finlayson, D. Kabra, S. Albert-Seifried, M. Song, R. Havenith, G. Tu, W. Huck, R. Friend, The Influence of Side-Chain Position on the Optoelectronic Properties of a Red-Emitting Conjugated Polymer, Macromolecular Chemistry and Physics, 214 (2013) 967-974.

[17] R. Mueller, P. Kleinebudde, Comparison of a laboratory and a production coating spray gun with respect to scale-up, Aaps Pharmscitech, 8 (2007) E21–E31.
[18] Q. Ye, K. Pulli, Numerical and Experimental Investigation on the Spray Coating Process Using a Pneumatic Atomizer: Influences of Operating Conditions and Target Geometries, Coatings, 7 (2017).
[19] J. Tomes, C. Finlayson, Low cost 3D-printing used in an undergraduate project: an integrating sphere for measurement of photoluminescence quantum yield, European Journal of Physics, 37 (2016) 055501.
[20] http://www.spray-nozzle.co.uk/docs/default-source/default-document-library/whats-in-a-spray.pdf,
[21] C. McNeill, B. Watts, L. Thomsen, H. Ade, N. Greenham, P. Dastoor, X-ray microscopy of photovoltaic polyfluorene blends: Relating nanomorphology to device performance, Macromolecules, 40 (2007) 3263-3270.
[22] C. McNeill, S. Westenhoff, C. Groves, R. Friend, N. Greenham, Influence of nanoscale phase separation on the charge generation dynamics and photovoltaic performance of conjugated polymer blends: Balancing charge generation and separation, Journal of Physical Chemistry C, 111 (2007) 19153-19160.
[23] C. Hoth, R. Steim, P. Schilinsky, S. Choulis, S. Tedde, O. Hayden, C. Brabec, Topographical and morphological aspects of spray coated organic photovoltaics, Organic Electronics, 10 (2009) 587-593.
[24] O. Kettner, C. Finlayson, B. Friedel, The Potential of P3HT:3C-SiC Composite Structures for Hybrid Photovoltaics, Nanoscience and Nanotechnology Letters, 7 (2015) 56-61.
[25] A. Sepe, Z. Rong, M. Sommer, Y. Vaynzof, X. Sheng, P. Muller-Buschbaum, D. Smilgies, Z. Tan, L. Yang, R. Friend, U. Steiner, S. Huttner, Structure formation in P3HT/F8TBT blends, Energy & Environmental Science, 7 (2014) 1725-1736.
[26] X. Yang, A. Uddin, Effect of thermal annealing on P3HT:PCBM bulk-heterojunction organic solar cells: A critical review (Retracted article. See vol. 43, pg. 1468, 2015), Renewable & Sustainable Energy Reviews, 30 (2014) 324-336.
[27] C. McNeill, J. Halls, R. Wilson, G. Whiting, S. Berkebile, M. Ramsey, R. Friend, N. Greenham, Efficient polythiophene/polyfluorene copolymer bulk heterojunction photovoltaic devices: Device physics and annealing effects, Advanced Functional Materials, 18 (2008) 2309-2321.
[28] C. McNeill, A. Abrusci, I. Hwang, M. Ruderer, P. Muller-Buschbaum, N. Greenham, Photophysics and Photocurrent Generation in Polythiophene/Polyfluorene Copolymer Blends, Advanced Functional Materials, 19 (2009) 3103-3111.
[29] S. Miller, G. Fanchini, Y. Lin, C. Li, C. Chen, W. Su, M. Chhowalla, Investigation of nanoscale morphological changes in organic photovoltaics during solvent vapor annealing, Journal of Materials Chemistry, 18 (2008) 306-312.
[30] C. Finlayson, A. Whitney, Photophysical studies of poly-isocyanopeptide based photovoltaic blends, Journal of Physics D-Applied Physics, 43 (2010) 095501.
[31] S. Westenhoff, I. Howard, R. Friend, Probing the morphology and energy landscape of blends of conjugated polymers with sub-10 nm resolution, Physical Review Letters, 101 (2008) 016102.
[32] Y. Tamai, H. Ohkita, H. Benten, S. Ito, Exciton Diffusion in Conjugated Polymers: From Fundamental Understanding to Improvement in Photovoltaic Conversion Efficiency, Journal of Physical Chemistry Letters, 6 (2015) 3417-3428.
[33] F. Krebs, All solution roll-to-roll processed polymer solar cells free from indium-tin-oxide and vacuum coating steps, Organic Electronics, 10 (2009) 761-768.
[34] F. Krebs, S. Gevorgyan, J. Alstrup, A roll-to-roll process to flexible polymer solar cells: model studies, manufacture and operational stability studies, Journal of Materials Chemistry, 19 (2009) 5442-5451.
[35] J. Kettle, N. Bristow, D. Gethin, Z. Tehrani, O. Moudam, B. Li, E. Katz, G. Benatto, F. Krebs, Printable luminescent down shifter for enhancing efficiency and stability of organic photovoltaics, Solar Energy Materials and Solar Cells, 144 (2016) 481-487.

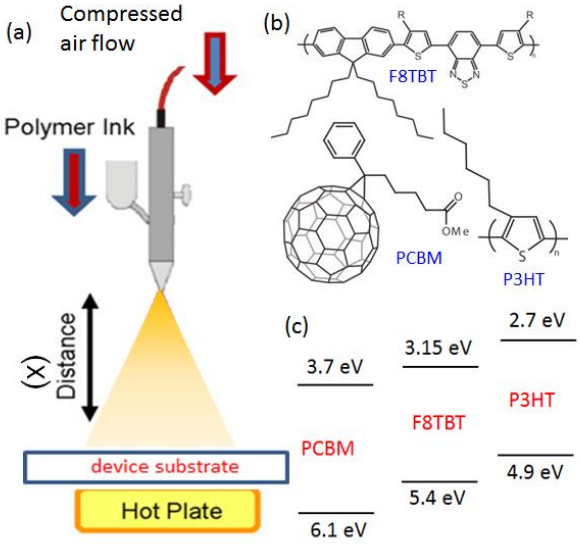

Figure 1; (a) schematic of spray-coating apparatus, illustrating the pneumatic spray-gun at working distance, x, from the heated substrate. (b) chemical structures of the materials used, namely PCBM, F8TBT, and P3HT. The inset below shows the interfacial energetics, illustrating the generic donor-acceptor nature of photovoltaic blends of the three semiconductors; given values of HOMO and LUMO are as taken from reference [15].

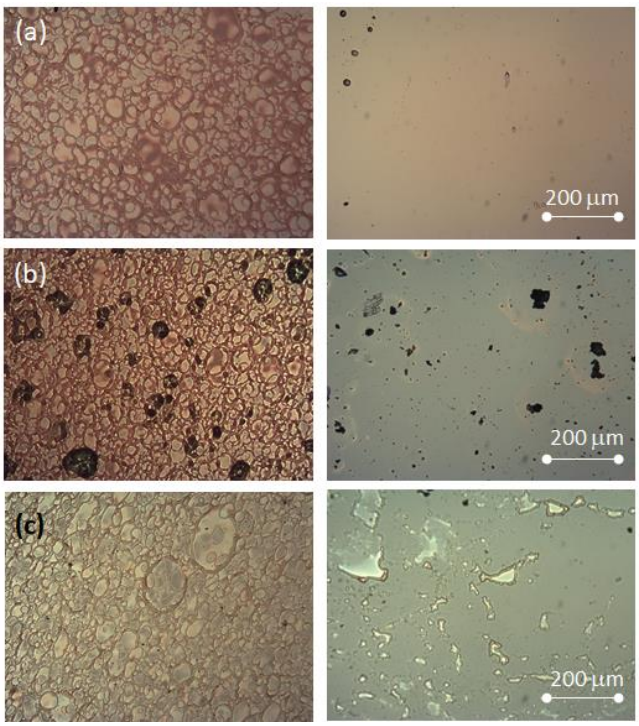

Figure 2; wide-area optical micrographs of 1:1 weight-ratio blend films derived from a DCB:CB 5:1 solvent medium, (a) P3HT/ F8TBT, (b) P3HT/PCBM, and (c) F8TBT/PCBM. On the left hand side, spray-coated films are shown, with typical film thicknesses of 150-200 nm, with three cycles of deposition (1 min total deposition, 30 sec dry time). Comparable spin-coated films are shown on the right hand side, with standard processing parameters of 1 mg/ml spun at 2000 rpm for 30 seconds onto spectrosil glass (Pi-Kem ltd, CS-05 unit).

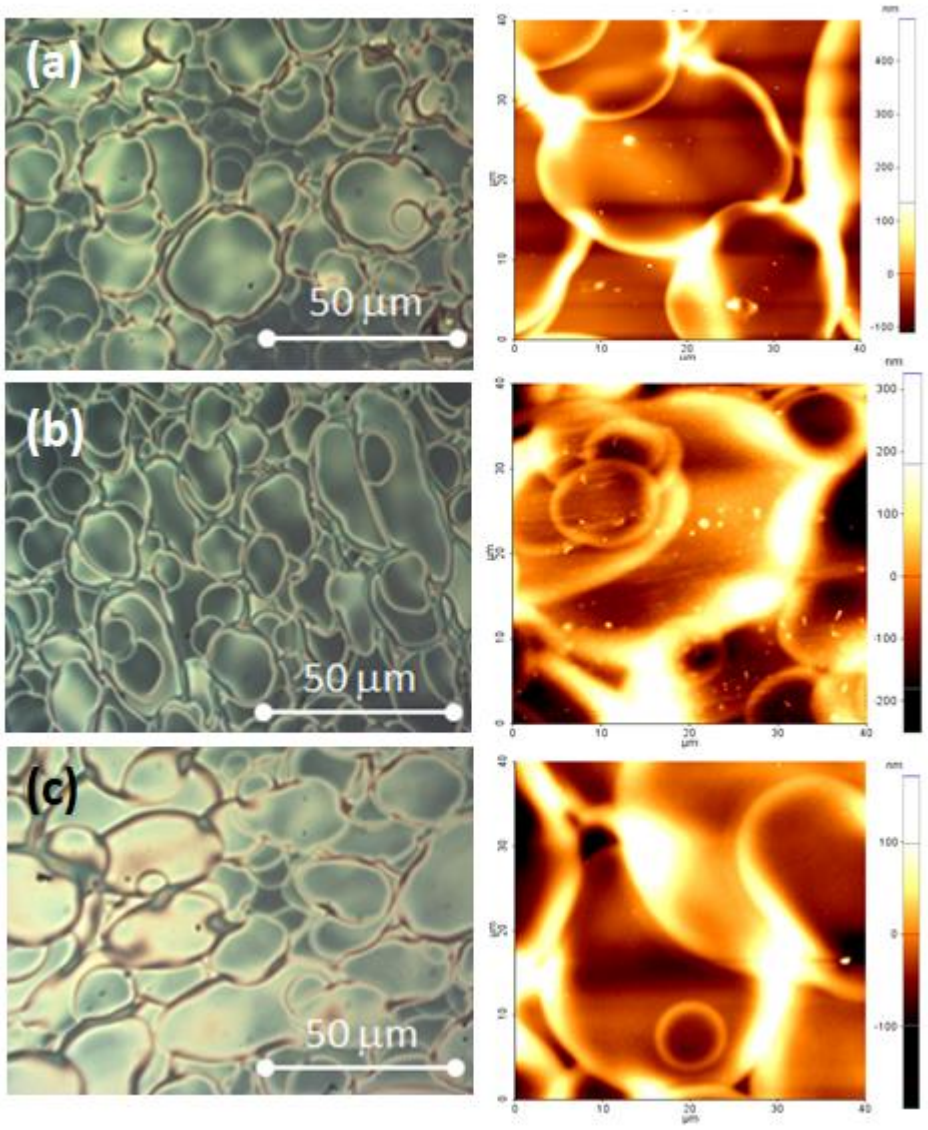

Figure 3; on the left are high-magnification optical micrographs of spray-coated 1:1 weight-ratio blend films from DCB:CB 5:1 solvent medium, (a) P3HT/ F8TBT, (b) P3HT/PCBM, and (c) F8TBT/PCBM. Right; atomic force micrographs (AFM) of equivalent samples covering 40 x 40 µm areas, with illustrative height-profile given for each micrograph.

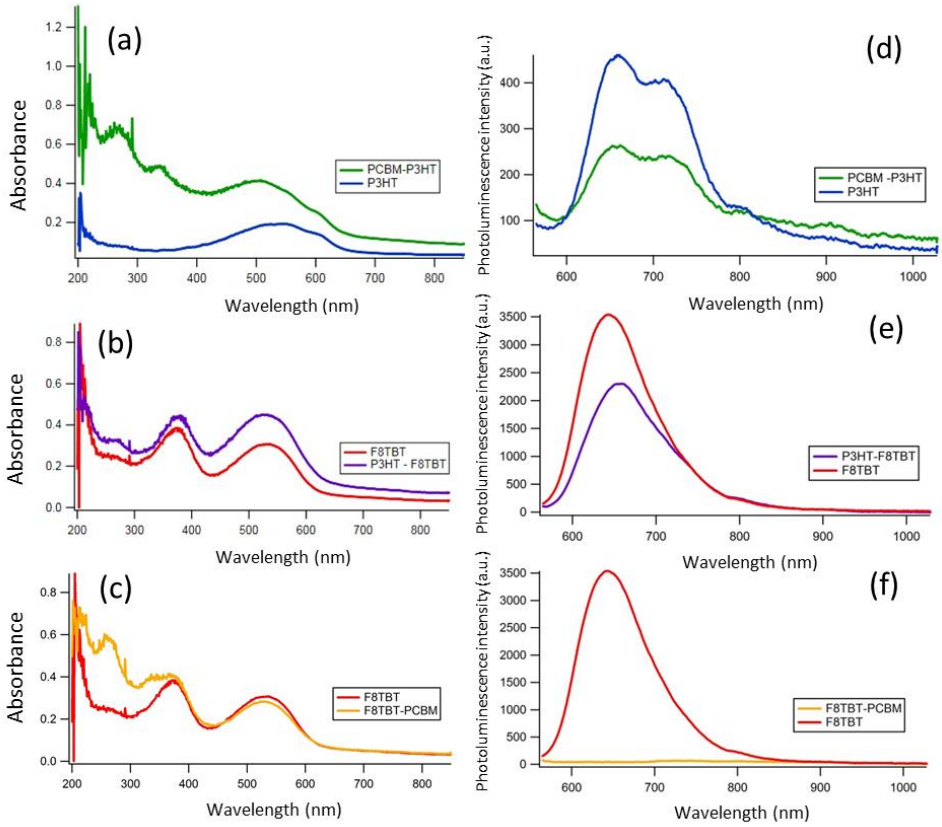

Figure 4; normalized optical absorption spectra of spray-coated 1:1 weight-ratio blend films from DCB:CB 5:1 solvent medium, in comparison to those deposited using a pristine material only; (a) P3HT/ F8TBT, (b) P3HT/PCBM, and (c) F8TBT/PCBM. Typical film thicknesses are 150-200 nm, three cycles of deposition (1 min deposition, 30 sec dry time). Corresponding normalized photoluminescence spectra for both pristine films and blends are shown in (d-f), as indicated.

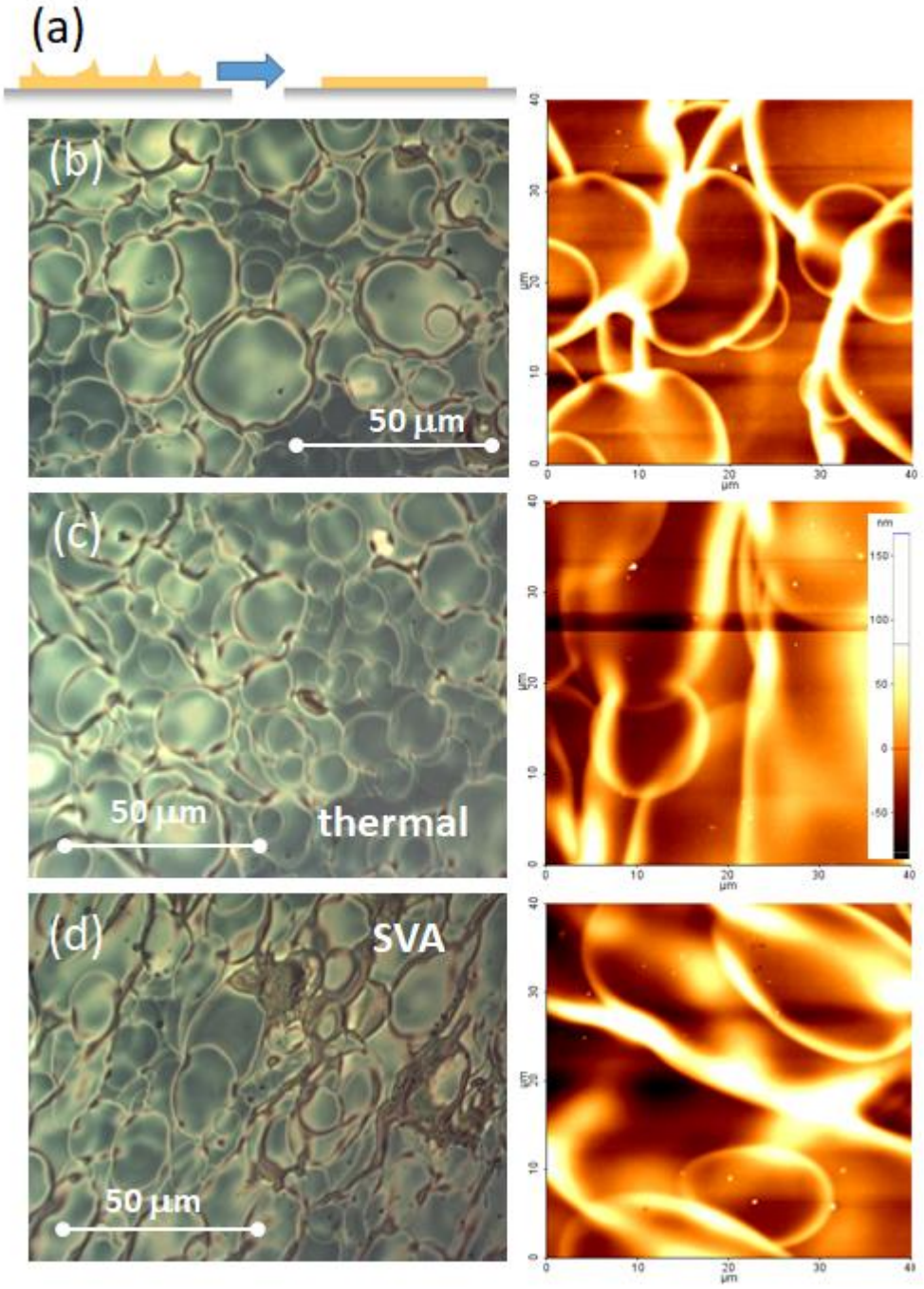

Figure 5; (a) schematic of possible effects of annealing on film planarity during thermal (melt) annealing. Optical (left) and AFM (right) micrographs below of P3HT/ F8TBT blend films, showing (b) the as deposited sample, (c) after thermal annealing treatment, and (d) after solvent-vapor annealing. AFM images are all displayed on 40 x 40 µm areas and on a common vertical scale height as shown in (c).

TABLES

Table 1; representative height-range profile and roughness statistics, as derived from AFM micrographs (such as those in Figure 2) of six samples for each blend/treatment permutation. Comparable roughness data following thermal annealing and solvent vapor annealing (SVA) are also given for comparison.

	P3HT/F8TBT	P3HT/PCBM	F8TBT/PCBM
Height range (nm)	108.6	101.2	95.3
r.m.s. roughness (nm)	49.9	92.1	39.0
After thermal annealing	28.0	50.7	34.4
After SVA	41.1	84.9	43.5

Table 2; photoluminescence (PL) quenching efficiencies (η) for as deposited blend films, together with comparable data following thermal annealing and solvent vapor annealing (SVA). Statistical errors are obtained from measurements of six samples for each blend/treatment permutation.

	P3HT/F8TBT	P3HT/PCBM	F8TBT/PCBM
PL-quenching efficiency (η, as deposited)	0.49 (±0.09)	0.77 (±0.08)	0.96 (±0.04)
η following thermal annealing	0.63 (±0.06)	0.80 (±0.04)	0.96 (±0.03)
η following SVA treatment	0.67 (±0.05)	0.88 (±0.03)	0.96 (±0.04)